
CONDENSED-GRADIENT BOOSTING

Seyedsaman Emami
Escuela Politécnica Superior
Universidad Autónoma de Madrid
Madrid
emami.seyedsaman@uam.es

Gonzalo Martínez-Muñoz
Escuela Politécnica Superior
Universidad Autónoma de Madrid
Madrid
gonzalo.martinez@uam.es

ABSTRACT

This paper presents a computationally efficient variant of Gradient Boosting (GB) for multi-class classification and multi-output regression tasks. Standard GB uses a 1-vs-all strategy for classification tasks with more than two classes. This strategy entails that one tree per class and iteration has to be trained. In this work, we propose the use of multi-output regressors as base models to handle the multi-class problem as a single task. In addition, the proposed modification allows the model to learn multi-output regression problems. An extensive comparison with other multi-output based Gradient Boosting methods is carried out in terms of generalization and computational efficiency. The proposed method showed the best trade-off between generalization ability and training and prediction speeds. Furthermore, an analysis of space and time complexity was undertaken.

Keywords Gradient Boosting Machine · Multi-output regression · Multi-class classification

1 Introduction

The field of machine learning has rapidly advanced in recent years, with numerous applications in a variety of industries. In particular, ensemble learning models have proven to be effective in solving multi-class classification [1, 2], multi-output regression problems [3, 4, 5], Multi-objective problems [6], and multi-task learning [7, 8]. Ensemble learning techniques consistently demonstrate exceptional robustness and accuracy [9, 10, 11], ranking them among the top-performing methods [12, 13]. Moreover, ensemble models exhibit superior performance in contrast to deep learning frameworks within model training and evaluation concerning tabular datasets, necessitating lesser tuning efforts [14]. Ensemble models leverage the combination of multiple base learners, typically weak individually, to create a robust learner. This fusion generally improves the generalization ability of its members.

One of the most renowned ensemble models is Gradient Boosting (GB), often referred to as Gradient Boosted Decision Trees (GBDT) [15]. In GB, the learning method works by sequentially creating new base models that learn the portion of the concept not 'captured' by previous learners. The problem is posed as an optimization-problem in which the output of each new model is built to be correlated with the negative gradient of the loss function of previous iterations. The current implementation of GB has both advantages and disadvantages, and significant improvements in this area have been achieved in recent years. For instance, in [16], a fast variant of GB was presented called XGBoost. XGBoost integrates a new regularization method into the objective function of gradient boosting and employs a fast strategy for decision tree splitting. This method drew much attention for achieving the best performance in many Kaggle competitions [16]. In a separate study, CatBoost tackles the prediction shift phenomenon observed during gradient boosting training by introducing a shifted permutation technique [17]. Moreover, CatBoost optimizes the training process, focusing particularly on categorical features. Furthermore, LightGBM [18] significantly advances Gradient Boosting techniques. It introduces two innovative methodologies: Gradient-based One-Side Sampling (GOSS) and Exclusive Feature Bundling (EFB). These methodologies are designed to address the inherent challenges in training speed encountered by earlier gradient boosting models, especially when dealing with large-scale datasets.

One limitation of the current gradient boosting approaches is that, for multi-class classification, it requires training one classifier for each class per iteration. That is, the model optimizes each class in a separate process. This approach can lead to substantial computational overhead, particularly when dealing with a large number of classes. Furthermore,

it often results in complex and slower ensembles. Moreover, for multi-output regression problems, it is required to build one isolated ensemble for each output, ignoring the correlations between the dependent variables. As the correlations between multiple outputs exist, [19] demonstrates that these correlations can enhance the performance of multi-output Support Vector Regression. Moreover, the complexity of existing ensemble models, particularly in the context of multi-class classification and multi-output regression, is a noteworthy concern. The conventional practice of training a separate classifier for each class in multi-class problems can lead to a proliferation of model components, significantly impacting computational demands. These large ensembles prolong both the training phase and prediction times [20, 21]. Furthermore, certain studies have proposed strategies to manage the computational demands of ensemble complexity. For instance, employing techniques like dimensionality reduction can expedite achieving the desired accuracy, as demonstrated by [22]. Alternatively, increasing computational resources may also be necessary. Hence, the imperative arises to develop less time complex and more fast ensembles [23]. Moreover, the extensive number of individual models can make both model interpretability and visualization more challenging. In the case of multi-output regression, the requirement to construct distinct ensembles for each output variable further exacerbates the issue. Each ensemble adds to the overall complexity, rendering the process of model management and optimization a challenging task. In addition to the interest in developing multi-output regression models capable of effectively incorporating the correlation between output targets in addition to input features [19, 24], it has been observed that ensemble variants of multi-output models exhibit very good performance across a large range of multi-output regression datasets, spanning disciplines from aerospace engineering and energy fields to environmental studies [25, 26, 5]. To address these challenges, it becomes imperative to explore strategies that streamline the training and prediction processes, while maintaining, or even enhancing, the overall model performance. The development and evaluation of Condensed-Gradient Boosting (C-GB), presented in this study, represents a step toward mitigating the complexities associated with current models and achieving more efficient solutions in multi-class classification and multi-output regression scenarios.

There are some proposals to use a single multi-output tree for all classes at each boosting iteration to produce faster ensembles. In cited works by [27, 28], the proposed methodologies are developed within the framework of gradient boosting, specifically leveraging the XGBoost algorithm and LightGBM. The two referenced studies employ the second-order Taylor expansion method to approximate their respective objective functions. Notably, the derivations are adapted to accommodate vectorized expressions of this expansion.

The objective of the current study has two parts. Firstly, it introduces a new GB model that addresses various problems uniformly, including binary/multi-class classification and single/multi-output regression. This is accomplished by employing a single model, potentially with multiple outputs, at each step. In contrast to [27, 28], the optimization of the proposed method is based on a two-step procedure. First, we fit the base learner by least-squares to the pseudo-residuals and then approximate the solution with the Newton-Raphson step following the original GB strategy [15]. The second objective of this paper is to perform an exhaustive comparison of multi-output GB methods in terms of generalization accuracy and computational efficiency.

The present paper's outline is as follows: Section 2 overviews relevant prior research. Section 3 explores the construction of Gradient Boosting, detailing the formulated objective function and algorithm designed for tackling multi-class classification and multi-output regression problems. Additionally, it provides illustrative examples to clarify the operational principles of the proposed model. In Section 4, the different subsections outline: the dataset utilized for the experiments, the code repositories corresponding to the studied models, the experimental setup, the evaluation metrics employed, the experimental methodology, and the results of various empirical analyses. Lastly, Section 5 summarizes the conclusions of the paper.

2 Related work

Several studies have proposed different extensions to boosting-like methods to better handle multi-class classification. These extensions are based on one of the two main families of boosting methods: AdaBoost [29, 30, 31] and Gradient Boosting (GB) [15, 32, 16].

The original AdaBoost [29] algorithm proposes two boosting variants to handle multi-class classification (called AdaBoost.M1 and M2). AdaBoost.M1 is based on using multi-class weak base learners, while AdaBoost.M2 converts the multi-class problem into a set of binary tasks. These multi-class versions could have theoretical and practical convergence problems [29, 33]. The work proposed in [33] tackles these problems by defining an exponential bound on a test measure called pseudo-loss error, in which each base learner (decision stumps in their work) minimizes its upper bound with gradient descent. Their method proved better convergence than AdaBoost.M2.

In multi-class tasks, the approach followed by Gradient Boosting [34] is to optimize a multi-class loss function separately for each class by training one tree per class. The main drawback of this approach is the complexity of the solution, as it involves generating a set of trees at each iteration.

In [35], an adaptive base class boosting (ABC-MART) is presented. The proposal derives the multi-class logistic regression loss function [15] given a sum-to-zero constraint, such that the sum of the outputs of the models adds up to zero. This allows them to choose, at each epoch, the base class which obtains the highest reduction of the training loss in a greedy manner. However, this greedy approach introduces higher training complexity in the algorithm.

The most similar studies to the present work are [27, 28]. The idea of those studies is the same as that of this work, which is to train a single tree for all classes at each boosting iteration, although they are based on a different optimization procedure. The work of [27] is based on XGBoost [16]. Their implementation, introduced as open-source based on TensorFlow, is named TFBT (stands for TensorFlow Boosted Trees) model. They showed how the use of a single multi-output regressor at each step produces less complex ensembles, reducing the size by approximately a factor of the number of classes. They introduced two strategies in terms of loss function calculation. One of them considers the full Hessian loss, and the other assumes that the Hessian matrix is diagonal, leading to a faster algorithm. Additionally, they included a layer-by-layer boosting methodology, characterized by incremental adjustments within the function space. In a similar approach, [28] introduced a Gradient-Boosted Decision Trees for Multiple Outputs (GBDT-MO) by training a single tree per iteration. The use of the objective function and its derivatives is the same as in [27]. Although GBDT-MO is implemented on top of LightGBM [18] and XGBoost objective function [16], they extended the histogram approximation of LightGBM for the multiple outputs, they also adapted the algorithm to multi-output regression and multi-class classification. These two studies ([27, 28]) consider the vector form of Taylor expansion to approximate their objective function, following the optimization procedure of XGBoost. Note that the original XGBoost and LightGBM also handle multi-output problems but build one tree per output per iteration, while the studies by [28] and [27] use a single tree per iteration. In contrast, our proposed model is a two-step optimization procedure that applies gradient descent and a Newton-Raphson step approximation to find the optimal solution, following the original GB approach. In the current study, we demonstrate that the proposed approach enhances generalization ability, training and prediction speeds, and model complexity.

A recent application of multi-output regression using gradient boosting involves predicting multi-step-ahead traffic speeds simultaneously [36]. Three distinct approaches were employed to address the multi-output regression in [36]. The first is an iterative strategy that uses predicted values for subsequent output predictions. The second approach is a direct strategy that constructs independent models for each output ignoring inter-output correlations. Lastly, the last strategy involved establishing a multivariable correlation matrix for prediction variables to compute correlation coefficients among sequences for each prediction step. This approach is then used to update the impurity function and consider all the outputs in the split finding.

Moreover, there are several implementations of multi-output decision trees, such as [37, 38]. The work presented in [37] is designed in the context of clustering. It uses a generic prototype distance function to maximize the inter-cluster distance in a standard top-down decision tree approach [39]. The functionality of their decision tree varies based on the selected prototype function, enabling its application in both classification and regression tasks. In [38], a constrained multi-output decision tree model is presented within the framework initially proposed. Their method entails the training of an extensive multi-output decision tree, followed by a pruning phase aimed at fulfilling specified user constraints pertaining to both size and accuracy. These multi-output decision trees can be combined into ensembles [40]. In [40], the multi-output decision trees of [38] are combined with bagging [41] and random forests [42]. The proposed ensembles [40] are tested on various classification and regression tasks, showing better performance than the single base models. Moreover, in the experiments carried out, the proposed multi-objective ensemble performed better on regression tasks than the single-objective ensembles. In classification, the performance of the multiple and single-output models was equivalent.

In a recent study by [43] a deep tree-ensemble (DTE) model is proposed. DTE approach entails constructing an ensemble of multiple layers of random forests (referred to as deep forest), with each layer enriching the initial feature set through the incorporation of a representation learning component based on tree embeddings. The DTE model is specifically developed for multi-output regression and multi-class classification tasks. Our proposed model diverges from the approach presented in [43]. We utilize multi-output decision tree regressors trained in an additive manner. In [4], a novel multi-output regression training procedure for shallow neural networks based on gradient boosting is proposed. This procedure demonstrates promising performance in terms of accuracy for multi-output regression tasks. Moreover, that study is extended in [5] proposing an ensemble of multi-output regression deep neural networks. The experimental results show that the proposed deep model achieves better generalization accuracy across various multi-output regression problems with respect to the shallow models. In the current paper, a multi-output decision tree

regressor is introduced as the additive model within gradient boosting, instead of using hidden unit of a shallow neural network. This approach produces simpler and faster to train models.

3 Methodology

This section discusses the Gradient Boosting (GB) algorithm, considering a dataset $D = \{(\mathbf{x}_i, y_i)\}_{i=1}^N$ drawn from a distribution $\mathcal{D} = \{\mathcal{X}, \mathcal{Y}\}$ where $\mathcal{X} \in \mathbb{R}^P$ and $\mathcal{Y} \in \mathbb{R}^K$ refer to a P -dimensional feature space and a K -dimensional output space, respectively. The algorithm is reviewed based on the Greedy function approximation [15] (Subsection 3.1). Furthermore, proposed modifications to handle multi-class classification by considering all classes simultaneously at each step, as well as outputs for multi-output regression are described (Subsection 3.2). In this study, M represents the total count of boosting epochs, with m serving as the index variable for individual boosting epochs within each iteration.

3.1 Gradient Boosted Decision Trees

In order to build the functional relationship between \mathbf{x}_i and y_i as $\hat{F}(x)$, that minimizes a given loss function (L)

$$\hat{F}(\mathbf{x}) = \operatorname{argmin}_{F(\mathbf{x})} \mathbb{E}_{\mathbf{x}, y} [L(y, F(\mathbf{x}))], \quad (1)$$

where \mathbb{E} is the expected value over the joint distribution, the optimization procedure followed by GB consists of estimating the objective function through an additive expansion

$$\hat{F}(\mathbf{x}) = \sum_{m=0}^M \gamma_m h_m(\mathbf{x}),$$

where $h(\mathbf{x})$ is a base regressor model. The model, $\hat{F}(\mathbf{x})$, is created in a stagewise greedy process as

$$(\gamma_m, h_m) = \operatorname{argmin}_{\gamma, h} \sum_{i=1}^N L(y_i, F_{m-1}(\mathbf{x}_i) + \gamma h_m(\mathbf{x}_i)), \quad (2)$$

and

$$F_m(\mathbf{x}) = F_{m-1}(\mathbf{x}) + \nu \gamma_m h_m(\mathbf{x}), \quad (3)$$

where ν is the learning rate hyperparameter that is useful for regularizing the model. In order to optimize Eq. (2), first the model h is trained, and then the value of γ is optimized. At each step, a gradient descent step is performed by computing the negative gradient, or pseudo-residuals, for each data point

$$r_{\{i, m\}} = - \left[\frac{\partial L(y_i, F(\mathbf{x}_i))}{\partial F(\mathbf{x}_i)} \right]_{F(\mathbf{x})=F_{m-1}(\mathbf{x})}. \quad (4)$$

The m -th decision tree regressor model, $h_m(\mathbf{x})$, is trained to adjust to the pseudo-residuals or gradients. Note that the gradients are optimized using a constrained function h , usually a decision tree, that is built using the square loss regardless of the loss function we are trying to optimize

$$h_m = \operatorname{argmin}_h \sum_{i=1}^N (r_{im} - h(\mathbf{x}_i))^2. \quad (5)$$

Hence, γ is subsequently optimized on the original loss function

$$\gamma_m = \operatorname{argmin}_{\gamma} \sum_{i=1}^N L(y_i, F_{m-1}(\mathbf{x}_i) + \gamma h_m(\mathbf{x}_i)). \quad (6)$$

The approximation is performed using a Newton-Raphson step. When the model h is a decision tree, this line search optimization can be done independently for each terminal leaf, because a decision tree can be seen as an additive model of the outputs of the terminal regions: $h_m(\mathbf{x}_i) = \sum_{j=1}^J b_{mj} \mathbb{I}(\mathbf{x}_i \in \mathbb{R}_j)$, where J is the number of terminal

nodes of the tree, \mathbb{R}_j is the region covered by leaf j and b_j is its output. The terminal regions are disjoint and cover the whole data space. Consequently, a different γ value can be computed for each terminal node j . We can integrate the general γ constant in each node as $\gamma_{\{m,j\}} = \gamma_m b_{\{m,j\}}$. With this, in the cases of binary classification or single-output regression in which one decision tree is built at each m iteration, the output of the leaf nodes is updated as

$$\gamma_{\{m,j\}} = \underset{\gamma}{\operatorname{argmin}} \sum_{\mathbf{x}_i \in \mathbb{R}_{\{m,j\}}} L(y_i, F_{m-1}(\mathbf{x}_i) + \gamma), \quad (7)$$

Note that for regression problems in which the square loss is optimized, this last step is not necessary as the leaf nodes already have the correct output.

Recent versions of Gradient Boosting include randomization hyperparameters that help its generalization performance and serve as a regularization mechanism [44]. These randomization techniques include data subsampling and feature subsampling for split finding.

3.2 Condensed Gradient Boosting

For the case of multi-class classification, since the base decision tree regressors supply scalar values, gradient boosting ensemble needs to build one tree per class and iteration. In this subsection, we derive the extension needed for GB [15] to work with a single decision tree regressor with vector-size outputs for multi-class classification and multi-output regression. One of these trees could replace the single-output trees used in standard GB. Considering a dataset as $D = \{(\mathbf{x}_i, y_i)\}_{i=1}^N$ and selecting a multi-class label with K class labels $k \in [1, K]$ sampled from the \mathcal{D} distribution, a one-hot encoding approach is employed to transform the multi-class labels into a logical matrix. In this matrix, each row i represents a vector of $y_{\{i,k\}}$, where $y_{\{i,k\}}$ equals 1 if the i -th instance belongs to class k , and 0 otherwise. The objective is to find K functions $\mathbf{F} = \{F_k\}_{k=1}^K$ that minimize a given loss function in an additive manner using multi-output models

$$\mathbf{F}_m(\mathbf{x}) = \mathbf{F}_{m-1}(\mathbf{x}) + \nu \tilde{\mathbf{h}}_m(\mathbf{x}) \quad (8)$$

where $\tilde{\mathbf{h}}_m(\mathbf{x}) = \{\gamma_{\{k,m\}} h_{\{k,m\}}(\mathbf{x})\}_{k=1}^K$ is the multi-output model with K outputs, and ν is the learning rate hyperparameter. Using the one-hot encoded class labels, at each iteration, a single multi-output tree is trained to fit the data in which the values to learn are a matrix of size $N \times K$ with the residuals of the previous predictions

$$r_{\{i,k,m\}} = - \left[\frac{\partial L(y_{\{i,k\}}, F_k(\mathbf{x}_i))}{\partial F_k(\mathbf{x}_i)} \right]_{F_k(\mathbf{x}) = F_{\{k,m-1\}}(\mathbf{x})}. \quad (9)$$

For node j with a vector of K outputs of the decision tree regressor, the criterion to minimize forthcoming splits is the average of Mean Squared Error (MSE) over the K outputs,

$$Q(j) = \frac{1}{N_j K} \sum_{k=1}^K \sum_{\mathbf{x}_i \in \mathbb{R}_j} (y_{ik} - \bar{y}_k)^2, \quad (10)$$

where \bar{y}_k is the mean value of target k in the region j , and N_j is the number of samples of node j .

As previously described (see Subsection 3.1), when the loss function is different from the one used when fitting the model to the matrix of residuals (as given by Eq. (10)), a second optimization step has to be carried out as in Eq. (7). In this second step, the K -dimensional vector of outputs of the leaf nodes has to be updated as

$$\gamma_{\{m,j,k\}} = \underset{\gamma}{\operatorname{argmin}} \sum_{\mathbf{x}_i \in \mathbb{R}_j} L(y_{ik}, F_{mk}(\mathbf{x}_i) + \gamma). \quad (11)$$

For multi-class classification, if log-loss is used

$$L(\mathbf{y}, \mathbf{F}(\mathbf{x})) = \sum_{k=1}^K y_k \ln \left(\frac{\exp(F_k(\mathbf{x}))}{\sum_{k=1}^K \exp(F_k(\mathbf{x}))} \right), \quad (12)$$

the Newton-Raphson update for tree terminal leaves would be

$$\gamma_{\{m,j,k\}} = \frac{\sum_{\mathbf{x}_i \in \mathbb{R}_j} r_{\{i,k,m\}}}{\sum_{\mathbf{x}_i \in \mathbb{R}_j} ((y_{\{i,k,m\}} - r_{\{i,k,m\}}) \times (1 - (y_{\{i,k,m\}} + r_{\{i,k,m\}})))}, \quad (13)$$

using the first-order derivative of the loss function (see Eq. (13)) near a given starting point to generate a sequence of improved approximations to the root of the objective function. For multi-output regression, if the square loss is used, there is no need to update the terminal vector values since the trees are already optimizing the desired loss function. The difference with a standard model would be that in the proposed algorithm all multiple regression outputs are learned and predicted using one tree per iteration and a single ensemble. The pseudo-code for the proposed method is succinctly delineated in Algorithm 1.

Algorithm 1 Condensed Gradient Boosting

- 1: **Input:**
 - Training dataset $D = \{(\mathbf{x}_i, y_i)\}_{i=1}^N$.
 - Loss function selection L .
 - Number of boosting rounds M .
 - Learning rate ν .
 - 2: **Output:**
 - Trained multi-output Condensed-Gradient Boosting $\mathbf{F}_m(\mathbf{x})$.
 - 3: Initialize $\mathbf{F}_0(\mathbf{x})$.
 - 4: **for** $t = 1$ to M **do**
 - 5: Compute the negative gradient.
 - 6: Fit the multi-output learner (\mathbf{h}_m) to the negative gradient Eq. (9).
 - 7: Create splits that minimize the L using Eq. (10).
 - 8: Update terminal regions of \mathbf{h}_m using Eq. (13).
 - 9: Update the ensemble multi-output model using Eq. (8).
 - 10: **end for**
-

3.3 Illustrative examples

Below, we include various examples to demonstrate the working mechanisms of the proposed C-GB model and standard GB in multi-class classification. In the first experiment, we analyzed the boundaries of GB and C-GB to compare whether creating a single multi-output regressor tree instead of one tree per class could pose difficulties in learning the concepts. For this experiment, a synthetic multi-class classification dataset with three class labels, 1200 instances and two input features is used. The generated dataset is based on the Madelon random data experiment [45]. The distribution of the training data points is shown in Figure 1 with each class in a different color. The same hyperparameter configuration is used for both methods (max depth=3, subsample=0.75, learning rate=0.1, and boosting iterations=100). In Figure 1, the decision boundaries of the two methods are shown using the same colors as the corresponding training data points. As evident from the subplots in Figure 1, both C-GB (subplot a) and GB (subplot b) exhibit remarkably similar performance and adeptly adapt to the training instances. This demonstrates the efficacy of the proposed method in adapting to the specific problem, despite training only one tree per iteration.

In Figure 2, the decision trees of the first iteration are shown as an example of the classification task shown in Figure 1. The figure displays individual trees per class for GB and a single tree for C-GB, specifically for iteration one. The tree nodes display various values: split information for internal nodes, MSE error of the node, the number of instances, and the node output. In multi-output decision tree (Figure 2 subplot a), the MSE represents the average error across all outputs (as per Eq. (10)), and the output value is a vector containing K classes. Figure 2 (subplot a) illustrates how a single tree can manage to capture the information of the three classes. The split of the root node and the left branch is equivalent to the class 0 tree of GB (Figure 2 subplot b), and isolates the class 0 (purple dots in Figure 1) from the rest. After the root node, the first two right nodes of the C-GB tree have the same splits as the first nodes of the second class of GB tree (Figure 2 subplot c). This illustrates how a single tree is able to capture the information of all classes in the problem in a more compact way (refer to Figure 2 subplot a). Also, using a single tree would produce more coherent outputs as the same splits are used for all classes.

To explore more the performance of C-GB and GB, we analyzed their convergence concerning the number of trees. This assessment is conducted on the *Waveform* dataset, focusing on the three class labels. The experiments are repeated 10 times, and the average values are reported. The hyperparameters used are: learning rate is set to 0.1 and the subsampling rate to 0.75. The convergence for each class is measured using average precision (i.e. true positives divided by detected positives) for each class. The results in average precision are shown in Figure 3 for various maximum depths (2, 5, 10, and 20 tree depths, arranged in ascending order from top to bottom) for both C-GB (blue curve) and GB (red curve). From Figure 3, it can be observed that both methods achieve equivalent precisions for all

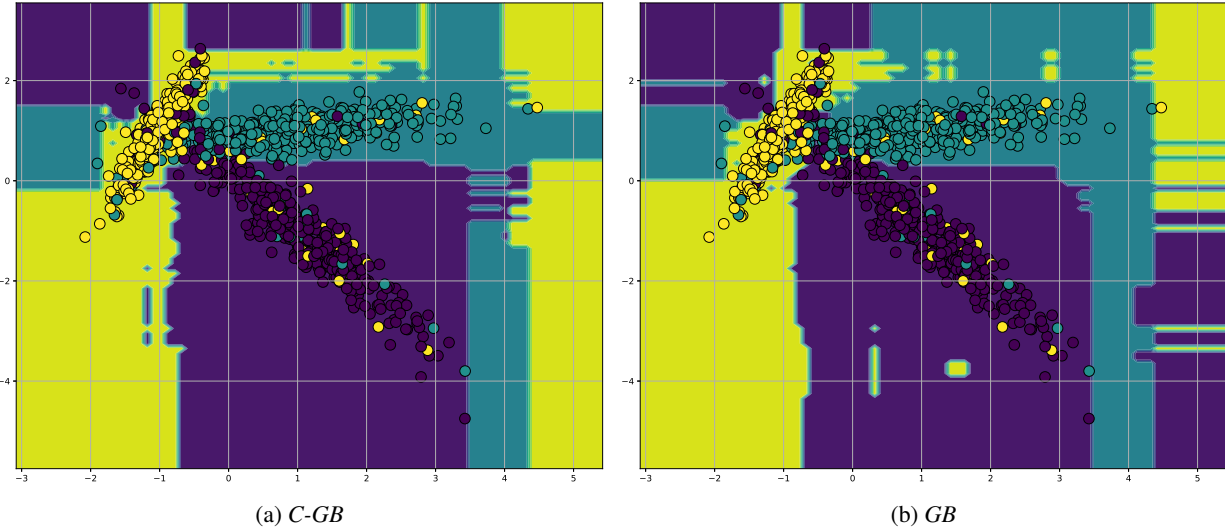


Figure 1: Classification boundaries for the C-GB (subplot a) and GB models (subplot b)

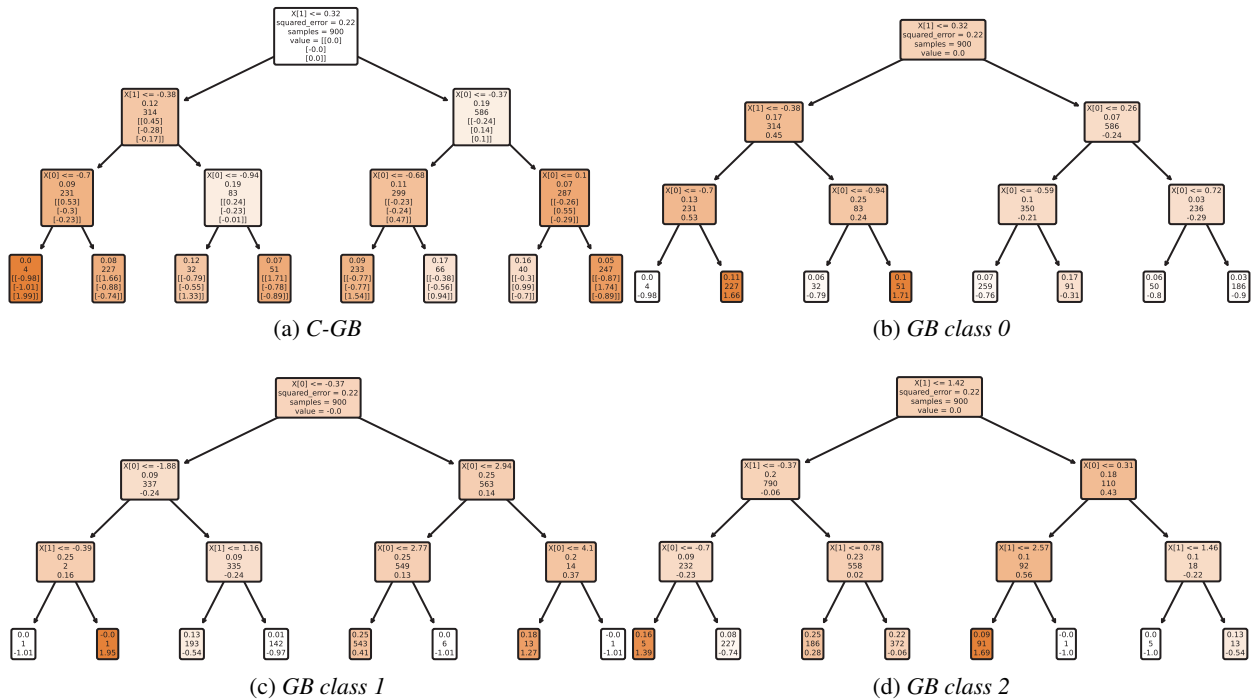


Figure 2: Decision tree regressors for the C-GB (a), class zero of GB (b), first class of GB (c), and last class of GB (d) for a multi-class classification problem with three classes

configurations. Even for the smaller depths, the final precision of both GB and C-GB are almost identical although the convergence for C-GB is a bit slower in this case.

4 Experiments

In this section, we carry out an exhaustive comparison of the proposed C-GB with respect to other similar algorithms such as TFBT [27] and GBDT-MO [28]. In addition, the comparison is extended to single-output gradient boosting

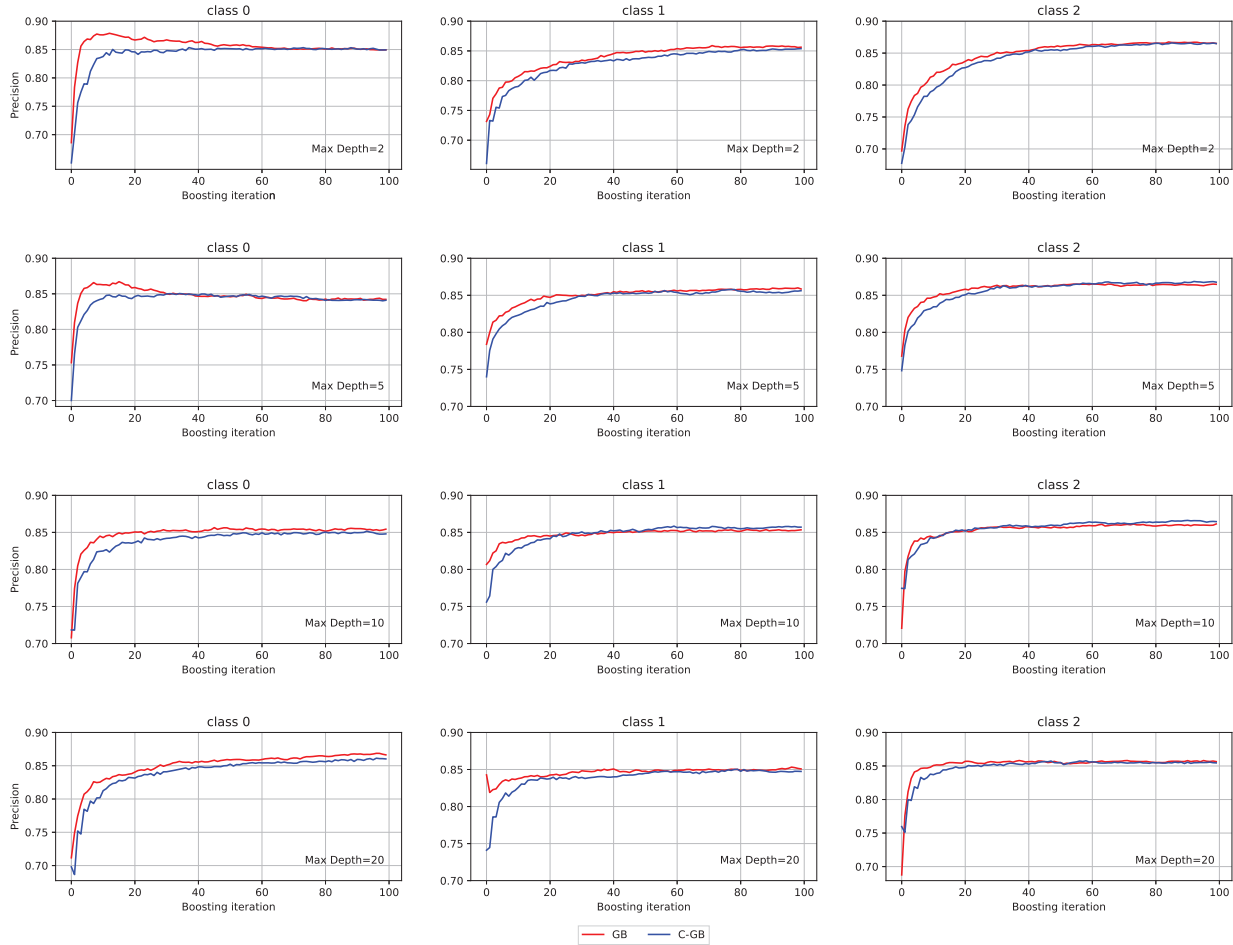


Figure 3: The precision curves for C-GB (blue) and GB (red) are depicted for each class across boosting epochs, showcasing the impact of varying maximum depth values on the decision tree

(GB). The analyses are performed on 12 multi-class classification and three multi-output regression tasks from diverse areas of application, each with a different number of instances, classes, and attributes. The details of the datasets are shown in Table 1. We selected these datasets in order to encompass significant variation in terms of different dimensions (samples and features), as well as the number of classes and targets.

The code of the proposed method (C-GB) is implemented on top of the `scikit-learn` library and it is available in the GitHub repository ¹. For the single-output GB, we used the implementation provided by `scikit-learn`, (version 1.2 and older) ². For GBDT-MO, we utilized the implementation from the authors of the GBDTMO package ³, as referenced in [28]. The implementation of TFBT is based on TensorFlow ⁴. Note, however, that in the last update of TensorFlow, the TFBT package was marked as deprecated (version 2.8.0 and older). Hence, we used a previous version of TensorFlow (version 2.4.1) which was used in the corresponding study by [27]. The libraries created by the author of each method were used to faithfully replicate the results. Note that all these frameworks are similar in the sense that they all provide a python wrapper over a C/C++ implementation for the decision trees underneath, which is the most time consuming operation [18]. The libraries used by the tested methods are all very well optimized for speed, specially LightGBM and XGBoost [13].

¹github.com/GAA-UAM/C-GB

²github.com/scikit-learn

³github.com/zzd1992/GBDTMO

⁴git.kot.tools/tensorflow

Table 1: Dataset description

Dataset	# Samples	# Features	# Outputs	Training and test samples
Multi-class classification				
CIFAR-10 [46]	60,000	3,072	10	10,000 test, and 50,000 train
Cover Type [47]	581,012	54	7	116,203 test, and 464,809 train
Digits [47]	1,797	64	10	360 test, and 1,437 train
iris [47]	150	4	3	30 test, and 120 train
Letter-26 [47]	20,000	16	26	6,000, test and 14,000 train
MNIST [48]	42,000	784	10	8,400 test, and 33,600 train
Poker Hand [47]	1,025,010	15	10	25,010 test, and 1,000,000 train
Sensit [49]	98,528	100	3	19,705 test and 78,823 train
Vehicle [47]	846	18	4	170 test and 676 train
Vowel [47]	990	10	11	198 test and 792 train
Waveform [47]	5,000	21	3	1,000 test and 4000 train
Wine [47]	178	13	3	36 test and 142 train
Multi-output regression				
ATP1d [25]	337	411	6	68 test and 269 train
ATP7d [25]	296	411	6	60 test and 236 train
Energy efficiency [47]	768	8	2	154 test and 614 train

4.1 Compared methods

The detailed definition of each of the algorithms included in the comparison and their differences from our proposed method are described in this subsection. Both the TFBT [27] and GBDT-MO [28] methodologies are developed on top of the XGBoost [16] framework. They both iteratively refine the optimization of a common objective function (see Eq.(14)). These methodologies are designed to manage multi-output decision trees at each epoch (\mathbf{h}_m), with \mathbf{b}_j representing their vector size leaf (j) output, given a designated loss function (L)

$$\mathcal{L}_m = \sum_{i=1}^N \left[L(\mathbf{h}_m(\mathbf{x}_i), \mathbf{y}_i) + \mathbf{G}_i \mathbf{b}_{\{m,j\}} + \frac{1}{2} \mathbf{H}_i \mathbf{b}_{\{m,j\}}^2 \right] + \Omega(\mathbf{b}_{\{m,j\}}), \quad (14)$$

where, \mathbf{G}_i and \mathbf{H}_i denote the first and second-order derivative of the loss function L with respect to the decision tree outputs ($\mathbf{b}_{\{m,j\}}$), respectively, and Ω represents the ensemble regularizer, designed to penalize the quantity of tree leaves as well as the L_2 norms of their respective weight vectors located at the leaf nodes.

The disparities between TFBT and GBDT-MO stem from their distinct implementations in programming paradigms. TFBT extends XGBoost’s foundational architecture⁵, while GBDT-MO is constructed atop the LightGBM library⁶.

4.2 Experimental setup

The validation procedure was carried out using random splits with the proportion of 20 percent for the test and the rest for the training sample, except for the *CIFAR-10*, *Poker Hand*, *MNIST* and *Sensit* for which the partition determined by the datasets was used. In order to have stable results, all experiments were repeated five times with different seed values except for the largest datasets: *CIFAR-10*, *MNIST*, *Sensit*, *Poker Hand*, and *Cover Type* in which only one experiment was performed. The reported generalization performance is computed as the average value of the different realizations. The size of the training and test sets for each dataset is indicated in the last column of Table 1. In an effort to achieve the highest possible accuracy performance for each model, the hyperparameters of each model were tuned using the grid-search method. This process involved conducting a grid search within the training phase employing 2-fold cross-validation across all models and datasets. The combination of hyperparameters yielding the best validation results was selected to train the final model of each algorithm on the complete training dataset. Table 2 displays the hyperparameter fixed values and grids for each model. It should be noted that all models are configured with boosting iterations.

⁵github.com/dmlc/xgboost

⁶github.com/microsoft/LightGBM

Table 2: Hyperparameter grid reporting variable configurations and predetermined values across diverse models

Model	Hyperparameter	Model	Hyperparameter	Model	Hyperparameter
C-GB	Tree depth	[-1, 2, 5, 10, 20]	GB	Tree depth	[-1, 2, 5, 10, 20]
	learning rate	[0.025, 0.05, 0.1, 0.5, 1]		learning rate	[0.025, 0.05, 0.1, 0.5, 1]
	max features	[sqrt, None]		max features	[sqrt, None]
	subsample	[0.75, 0.5, 1]		subsample	[0.75, 0.5, 1]
TFBT	Tree depth	[2, 5, 10]	GBDT-MO	Tree depth	[2, 5, 10, 20]
	learning rate	[0.025, 0.05, 0.1, 0.5, 1]		learning rate	[0.025, 0.05, 0.1, 0.5, 1]
	subsample	[1]		subsample	[0.75, 0.5, 1]

In addition to the generalization performance, the training and prediction times were also measured. In training, only the time (in seconds) necessary to train the models was logged without considering the time required to load the data in memory. The prediction time was computed as the average time each model needs to predict 10^5 instances. It is important to note that the training time depends on the hyperparameter configuration. To ensure consistency across models, we considered employing the same set of hyperparameters for all models. These included subsample = 1, learning rate = 0.1, max depth = 10, and boosting iteration = 100. In addition, the complexity of the different models was conducted using big \mathcal{O} notation, which is independent of the programming language of the implementation. This measurement evaluates how the runtime and disk space consumption of an algorithm increase relative to the input size and significant hyperparameters. It provides an upper limit on the worst-case scenario for both runtime and space requirements. It is important to note that all experiments were conducted utilizing an Intel(R) Xeon(R) CPU featuring six cores and operating at a base clock rate of 2.40GHz.

4.3 Evaluation

The generalization ability of the different algorithms in the classification tasks was assessed using the accuracy of the models. For the multi-output regression problems, the root mean square error ($RMSE$) was used for each individual output,

$$RMSE_k = \sqrt{\frac{\sum_{i=1}^N (y_{ik} - \hat{y}_{ik})^2}{N}},$$

where y_{ik} and \hat{y}_{ik} are the target true and predicted values respectively. Furthermore, to have a unique performance criterion for each model in the multi-output regression tasks, we considered the average coefficient of determination, aR^2 over K outputs

$$aR^2(y_{ik}, \hat{y}_{ik}) = \sum_{k=1}^K \left(1 - \sum_{i=1}^N \frac{(y_{ik} - \hat{y}_{ik})^2}{(y_{ik} - \bar{y}_k)^2} \right) / K,$$

where \bar{y} is the mean of the observed values y_i , the highest possible value for aR^2 is 1.0. Negative values indicate poor performance, worse than predicting the average of the real target values for all test instances. We did not consider the average $RMSE$ over all the targets as it would be an average of values on different units, making it difficult to interpret.

Finally, in order to compare the performance across datasets and methods, the statistical ranking methodology proposed by Demsar [50] was applied. This methodology computes the average rank for each method across the tested datasets. The difference in average rank is considered significant using an Nemenyi test. The result of this test can be plotted using a Demsar [50] as shown in Figure 4. The ranking of the methods in each dataset was done using the average accuracy in the classification tasks. For the regression problems, the methods were ranked by target using the $RMSE$ metric.

4.4 Results

The average results for the different experiments are shown in Tables 3, 4, and 5. In Table 3, the average accuracy for the multi-class tasks is shown. Tables 4 and 5 show the average $RMSE$ and average R^2 -score for the multi-output regression problems. The tables show the comparative evaluation of the following methods: the proposed C-GB model, Standard single-output Gradient Boosting (GB), TFBT (only for classification), and GBDT-MO. The best value for each dataset or target is highlighted in the tables with a light blue shading.

Table 3: Average generalization accuracy for C-GB , GB, TFBT, and GBDT-MO. The best results are highlighted in a light blue hue

Dataset	C-GB	GB	TFBT	GBDT-MO
CIFAR-10	51.31	51.98	36.15	48.67
Cover Type	97.23	97.25	73.94	84.60
Digits	97.17	97.39	95.94	96.39
Iris	94.00	95.33	93.33	92.67
Letter-26	96.80	96.57	76.44	94.74
MNIST	97.48	97.63	80.48	96.71
Poker Hand	74.87	76.81	57.63	78.15
Sensit	84.83	85.07	75.47	82.95
Vehicle	75.06	75.06	64.24	72.12
Vowel	96.16	95.76	70.91	83.54
Waveform	85.12	85.24	80.00	84.40
Wine	98.89	97.78	92.78	86.67

Table 4: Average generalization RMSE for C-GB, GB, and GBDT-MO. The best results are highlighted in a light blue hue

Dataset Target	ATP1d						ATP7d						Energy	
	0	1	2	3	4	5	0	1	2	3	4	5	0	1
C-GB	51.98	107.79	79.58	51.74	61.99	59.48	25.39	68.86	55.72	39.03	33.34	41.22	0.37	0.94
GB	48.38	113.19	74.55	32.26	51.27	34.24	28.09	64.97	61.42	37.78	34.98	35.41	0.49	0.83
GBDT-MO	77.04	171.22	136.08	129.41	90.34	134.34	97.03	190.15	171.74	179.38	111.71	184.78	1.21	2.10

As shown in Table 3, GB generally exhibits an accuracy superior to that of the other models, achieving the highest accuracy in eight out of 12 datasets. The C-GB shows a rather good performance with four best performances. GBDT-MO obtained the best performance in one dataset, and TFBT did not achieve the best performance in any of the datasets. The disparity in performance between GB and its extension, C-GB, is generally marginal across most datasets. For example, in the *Waveform* dataset, the accuracy difference between these models is approximately 0.12, and in *Cover Type*, it is around 0.02. The most significant performance margin in favor of GB occurs in the *Poker Hand* dataset, with a notable difference of 1.94 points, coinciding with the dataset where GBDT-MO achieves its best result. C-GB demonstrates its highest performance in *Wine* and *Vowel*, surpassing GB by 1.11 and 0.4 points, respectively.

The results of the multi-output regression experiments are shown in Tables. 4 and 5. In this experiment, as GB does not support multi-output regression, we trained one different ensemble for each output separately. Results are not reported for TFBT as this method cannot handle regression tasks.

From Table. 4, it can be observed that the performance of C-GB and GB on each target are and superior to that of GBDT-MO. Specifically, GB achieves the optimal performance in nine targets, whereas C-GB demonstrates superiority in five. Conversely, GBDT-MO fails to achieve comparable performance to the other two methodologies. A similar trend is observed in the average R^2 score shown in Table 5. GB attains the highest score across all datasets, followed by C-GB.

In addition, the average performance of GBDT-MO in the *ATPID* dataset is clearly lower than that of the other two methods. To explore in the dynamics od this dataset, a scatter plot illustrating the correspondence between the predicted and actual values for each target is shown in Figure 5. The poor performance of GBDT-MO in this dataset can be attributed to its tendency to generate similar predictions for most instances.

Table 5: Average generalization coefficient of determination C-GB, GB-SO, GBDT-MO. The best results are highlighted in a light blue hue

Dataset	C-GB	GB	GBDT-MO
ATP1d	0.8210	0.8381	0.4567
ATP7d	0.6952	0.7203	-1.4765
Energy	0.9944	0.9982	0.9606

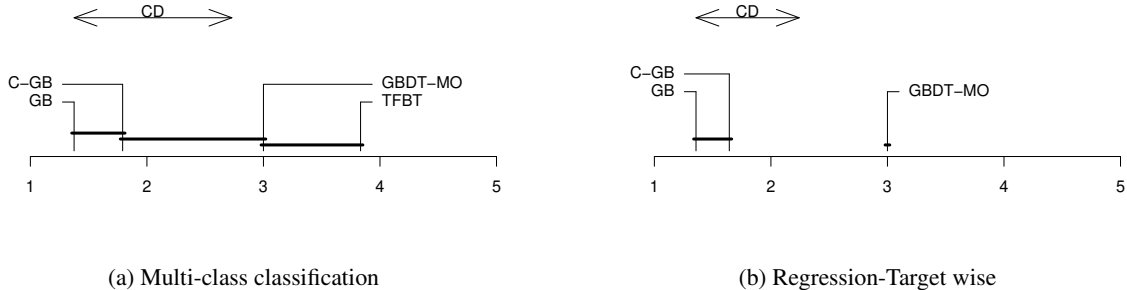


Figure 4: Comparison of different gradient boosting models (higher rank is better) using the Nemenyi Test, ($p = 0.05$)

Figure 4 shows the overall comparison of the tested methods using a Demsár diagram. The plots display the average rank of the methods for the analyzed datasets. The difference between the two methods is statistically significant if they are not connected with a horizontal solid line. The critical distances (CD) are 1.64 and 0.88 for 12 multi-class classification tasks and 14 regression targets, respectively with p -value = 0.05.

Similar conclusions can be drawn from these diagrams. For the multi-class classification problems (Figure 4 subplot a), the worse performance is produced by TFBT followed by GBDT-MO. The best average rank is achieved by GB followed by the proposed C-GB model. The performance of C-GB in multi-class classification is statistically significantly better than that of TFBT. As for the regression tasks (Figure 4 subplot b), we ranked, the models over 14 regression targets for three models. The best rank was achieved by the GB and C-GB with statistical significant difference in relation to GBDT-MO. It is noteworthy that GBDT-MO differs statistically from both C-GB and GB models.

One critical aspect of these methods is their computational complexity. To assess this aspect, two different analyses are employed. First, the training and inference (test) times of the studied models, are measured for all datasets. For this analysis the implementation of the authors was used for each method. Second, and in order to have a complexity analysis independent of their implementation, we carried out a second analysis based on big \mathcal{O} notation. With this analysis the time and space complexities of these models was explored.

The time performances are outlined in Table 6. The results of this table are generally more favorable to two methods based on multi-output trees: C-GB and GBDT-MO. C-GB trained faster in eight datasets, and the GBDT-MO trained faster in seven. In addition, the training times are generally favorable to C-GB in the largest datasets: for instance in *CIFAR-10* and *MNIST*, GBDT-MO is respectively 2528.42 and 861.12 seconds slower than the C-GB. The training times for GB are clearly slower than those of C-GB. Regarding the test time required to evaluate 10^5 instances, the GBDT-MO model was the fastest in nine datasets and C-GB in four. The results of GB, in this regard, are somewhat more competitive in small datasets, even though one tree per class and iteration has to be evaluated. The reason for this is that in general, the size of the decision trees generated by GB is smaller.

In relation to time complexity of the algorithms, we focus on the time required to fit the decision tree structure, where the most complex operations occur [18]. For that, we revisit the key parameters in our study: N represents the total number of samples, P denotes the number of input features and λ the depth of the trees. The time complexity for building a decision tree can be expressed in terms of the complexity of the split finding algorithm and the number of splits related to the depth. In this study, the various models differ in terms of the algorithms used to find the best splits. For CART-based decision tree splits, which are the trees used in GB and C-GB, the split algorithm consists of ordering the values of an attribute ($N \log_2(N)$) and then loop over it (N) to compute the gain of each possible split (this operation can be performed independently of the number of classes although there is a one time cost K of initialization). This is repeated for all attributes (P), so the complexity is $\mathcal{O}(P \times (N \log_2(N) + N + K)) = \mathcal{O}(P \times N \log_2(N))$, assuming $K \ll N$. Considering the data is divided in half after each split, we have that at the next depth $2 \times P \times N/2 \log_2(N/2)$ operations need to be done, which resolves to $\mathcal{O}(P \times N \times \log_2(N))$. Hence, the total cost for building a tree is $\mathcal{O}(P \times N \times \log_2(N) \times \lambda)$. On the other hand, GBDT-MO utilizes the LightGBM implementation and TFBT is based on XGBoost. Both LightGBM and XGBoost exhibit identical time complexity in split finding [28] characterized by $\mathcal{O}(\beta \times P \times K)$ where β is the number of bins employed within the split-finding histogram methodology. Further details and substantiation can be found in [28]. This splitting cost is the same for every level of the tree. Consequently, the cost for building a tree is $\mathcal{O}(\beta \times P \times K \times \lambda^2)$. This algorithm also has a one

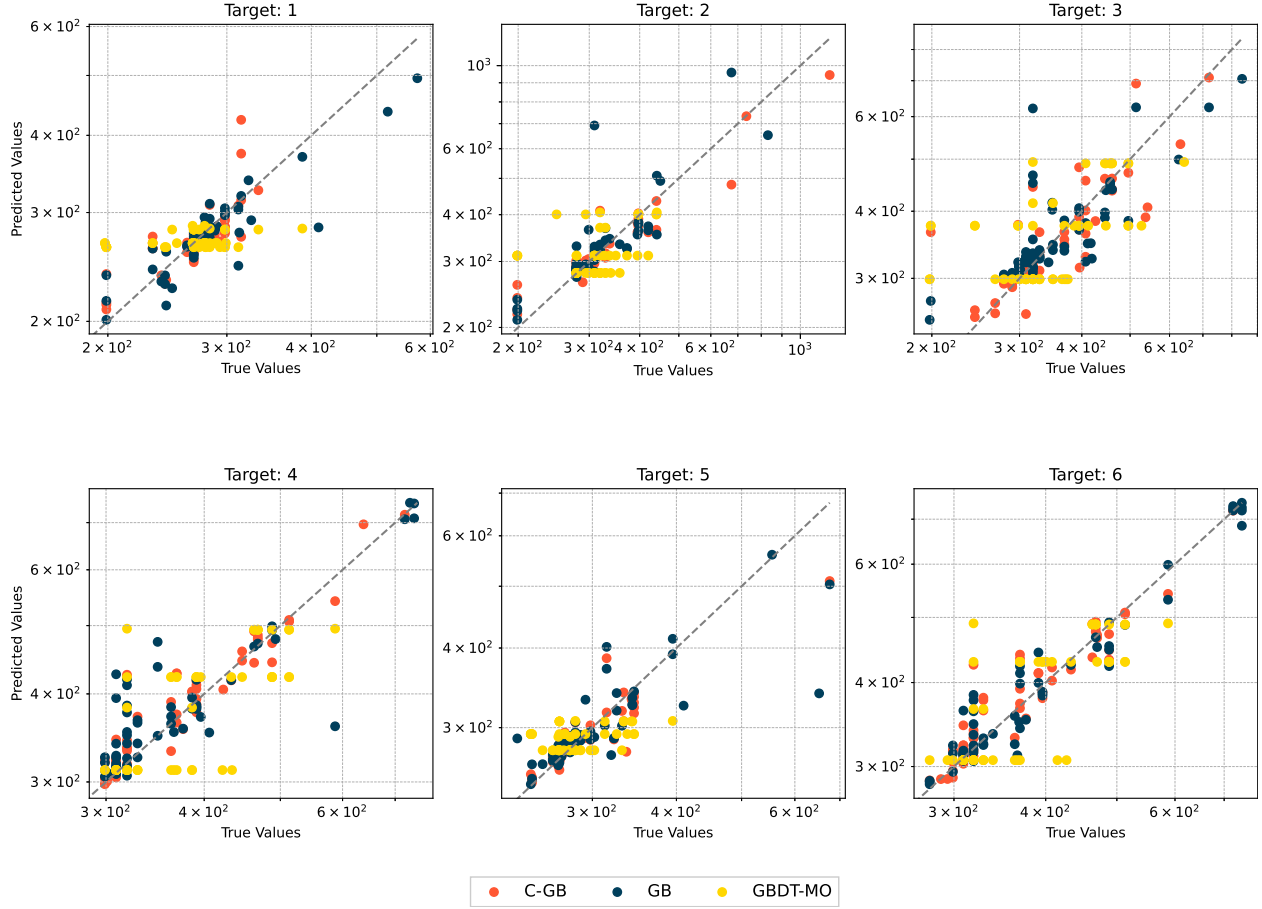


Figure 5: Scatter Diagram of Prediction: For six outputs of the ATP7D and three models: C-GB (red dots), GB (dark blue dots), and GBDT-MO (yellow dots)

time cost of $P \times N$ that is needed to compute the bins. With that said and recalling the number of boosting epochs (M) and classes (K), we can express the total time complexity of each analyzed model as shown in Table 7.

As shown in Table 7, the models based on bins ($\ll N$) have a better complexity with respect to GB and C-GB, specially for small depths (λ). In any case, depending on the selected hyperparameters selected for each model the actual training times could differ in practice.

To assess the space complexity of the studied algorithms, we outline three fundamental allocations necessary for training the models as follows:

- Storage of decision trees: $\mathcal{O}(M \times |h(\mathbf{x})|)$, where $\mathcal{O}(|h(\mathbf{x})|)$ is the tree size that is given by the number of nodes times the size of each node. The number of nodes is $\mathcal{O}(\lambda^2)$. The node size includes the split threshold, attribute index, pointers to the left and right nodes, and, for leaf nodes, the output values, which is a K -size vector. In consequence, the size of a tree is $\mathcal{O}(h(\mathbf{x})) = \mathcal{O}(\lambda^2 \times (K + \#node_params))$
- Gradient information: $\mathcal{O}(N \times K)$.
- A space reserve dedicated to housing histograms (specifically in the case of GBDT-MO and TFBT algorithms): $\mathcal{O}(\beta \times K)$.

This gives a space complexity of the analyzed models shown in Table 8. The space complexity of GB is the largest of the models, especially considering that the size required for the number of parameters of a tree node is usually larger than the number of classes.

In fact, one of the main benefits of multi-output models is their fast prediction speed, as illustrated in Table 6.

Table 6: Training and prediction time comparison (in seconds) for C-GB, GB, TFBT, and GBDT-MO. The best results are highlighted in light blue hue

Models Dataset	C-GB		GB		TFBT		GBDT-MO	
	Training	Prediction	Training	Prediction	Training	Prediction	Training	Prediction
Multi-class classification CIFAR-10	332.69	48.29	2274.58	42.60	138265.17	643.44	2861.12	8.42
Cover Type	249.86	1.55	1092.56	4.78	67268.82	7.51	345.41	3.46
Digits	2.72	5.51	14.07	19.16	1687.25	262.56	4.60	2.88
iris	0.18	32.38	0.35	19.21	26.11	1560.24	0.04	1.22
Letter-26	15.30	2.16	157.23	23.67	2399.45	16.75	13.78	3.72
MNIST	90.89	15.93	687.03	33.00	34392.61	173.45	952.02	5.81
Poker Hand	12.29	2.33	71.59	9.31	334.97	1.59	35.02	2.39
Sensit	132.23	2.17	325.21	2.64	2020.74	22.03	73.17	3.63
Vehicle	1.21	7.95	3.29	10.27	133.00	325.85	0.90	1.81
Vowel	2.06	7.94	10.98	25.26	390.70	277.87	1.13	2.22
Waveform	3.68	2.31	7.49	3.14	159.74	64.57	2.72	3.55
Wine	0.21	32.19	0.39	16.99	73.39	1281.90	0.10	0.99
Multi-output regression ATP1d	0.34	18.22	1.21	21.23			8.17	1.19
ATP7d	0.30	19.82	1.07	21.46			7.22	1.12
Energy	0.14	6.97	0.16	4.16			0.20	1.28

Table 7: Time complexity

Model	Time complexity
C-GB	$\mathcal{O}(M \times P \times N \times \log_2(N) \times \lambda)$
GB	$\mathcal{O}(K \times M \times P \times N \times \log_2(N) \times \lambda)$
TFBT	$\mathcal{O}(M \times \beta \times P \times K \times \lambda^2 + P \times N)$
GBDT-MO	$\mathcal{O}(M \times \beta \times P \times K \times \lambda^2 + P \times N)$

5 Conclusion

In this paper, Condensed Gradient Boosting (C-GB) is presented. C-GB is a variant of Gradient Boosting (GB) for multi-class classification and multi-output regression problems. In multi-class problems (i.e. tasks with more than two classes), GB has to train one regressor model per class and iteration. In this work, we proposed the use of decision trees with vector-valued leaves in such a way that only one decision tree per iteration has to be trained. We have shown that these multi-output regression trees are able to capture the information of all classes at once. In addition, the use of these trees allowed us to adapt the model to multi-output regression. The proposed method is implemented as an open-source package for further investigations. An extensive experimental comparison has been carried out. The proposed model has been compared with standard GB. Moreover, this comparison was extended to include two other similar multi-output models employing distinct optimization strategies: TFBT utilizing XGBoost and GBDT-MO employing LightGBM. The experiments showed that the proposed approach achieved a level of generalization performance comparable to that of the standard GB method, while decreasing the utilization of computational resources. The ensembles produced by C-GB generally outpace standard GB in training and prediction speed. Moreover, the proposed model exhibits superior generalization performance when compared to TFBT and GBDT-MO in the tested dataset. In computational terms, TFBT emerges as the slowest method, while GBDT-MO and C-GB stand out as the fastest among all tested techniques.

The proposed model’s performance has significant implications for real-world applications, particularly in terms of computational efficiency. Future research should prioritize assessing its compatibility with deep learning architectures

Table 8: Space complexity

Model	Space complexity
C-GB	$\mathcal{O}(M \times (\lambda^2 \times (K + \#node_params)) + N \times P \times K)$
GB	$\mathcal{O}(K \times M \times (\lambda^2 \times (2 + \#node_params)) + N \times P \times K)$
TFBT	$\mathcal{O}(M \times (\lambda^2 \times (K + \#node_params)) + N \times P \times K + \beta \times K)$
GBDT-MO	$\mathcal{O}(M \times (\lambda^2 \times (K + \#node_params)) + N \times P \times K + \beta \times K)$

as well as exploring techniques to handle imbalanced classes and high-dimensional feature spaces, common challenges in multi-class problems.

Acknowledgment

The authors acknowledge financial support from project PID2022-139856NB-I00 funded by MCIN/ AEI / 10.13039/501100011033 / FEDER, UE and project PID2019-106827GB-I00 / AEI / 10.13039/501100011033 and from the Autonomous Community of Madrid (ELLIS Unit Madrid). We also extend our appreciation to the Centro de Computación Científica CCC-UAM for providing computational resources.

References

- [1] Seyedsaman Emami and Gonzalo Martínez-Muñoz. A gradient boosting approach for training convolutional and deep neural networks. *IEEE Open Journal of Signal Processing*, 4:313–321, 2023.
- [2] Sohaib Asif, Ming Zhao, Xuehan Chen, and Yusen Zhu. Bmri-net: A deep stacked ensemble model for multi-class brain tumor classification from mri images. *Interdisciplinary Sciences: Computational Life Sciences*, 15(3):499–514, September 2023.
- [3] Cansel Kucuk, Derya Birant, and Pelin Yildirim Taser. An intelligent multi-output regression model for soil moisture prediction. In *Intelligent and Fuzzy Techniques for Emerging Conditions and Digital Transformation*, pages 474–481, Cham, 2022. Springer International Publishing.
- [4] Seyedsaman Emami and Gonzalo Martínez-Muñoz. Multioutput regression neural network training via gradient boosting. In *30th European Symposium on Artificial Neural Networks, Computational Intelligence and Machine Learning, ESANN 2022, Bruges, Belgium, October 5-7, 2022*, 2022.
- [5] Seyedsaman Emami and Gonzalo Martínez-Muñoz. Deep learning for multi-output regression using gradient boosting. *IEEE Access*, 12:17760–17772, 2024.
- [6] Zhiwen Yu, Yidong Zhang, CL Philip Chen, Jane You, Hau-San Wong, Dan Dai, Si Wu, and Jun Zhang. Multi-objective semisupervised classifier ensemble. *IEEE transactions on cybernetics*, 49(6):2280–2293, 2018.
- [7] Seyedsaman Emami, Carlos Ruiz Pastor, and Gonzalo Martínez-Muñoz. Multi-task gradient boosting. In *Hybrid Artificial Intelligent Systems*, pages 97–107, Cham, 2023. Springer Nature Switzerland.
- [8] Jae-Yeop Jeong, Yeong-Gi Hong, Sumin Hong, JiYeon Oh, Yuchul Jung, Sang-Ho Kim, and Jin-Woo Jeong. Ensemble of multi-task learning networks for facial expression recognition in-the-wild with learning from synthetic data. In *Computer Vision – ECCV 2022 Workshops*, pages 60–75, Cham, 2023. Springer Nature Switzerland.
- [9] Kun Li, Haocheng Xu, and Xiao Liu. Analysis and visualization of accidents severity based on lightgbm-tpe. *Chaos, Solitons & Fractals*, 157:111987, 2022.
- [10] Selçuk Demir and Emrehan Kutlug Sahin. Predicting occurrence of liquefaction-induced lateral spreading using gradient boosting algorithms integrated with particle swarm optimization: Pso-xgboost, pso-lightgbm, and pso-catboost. *Acta Geotechnica*, 18(6):3403–3419, June 2023.
- [11] Lakshmana Rao Namamula and Daniel Chaytor. Effective ensemble learning approach for large-scale medical data analytics. *International Journal of System Assurance Engineering and Management*, 15(1):13–20, 01 2024.
- [12] Chongsheng Zhang, Changchang Liu, Xiangliang Zhang, and George Almpanidis. An up-to-date comparison of state-of-the-art classification algorithms. *Expert Systems with Applications*, 82:128–150, 2017.
- [13] Candice Bentéjac, Anna Csörgő, and Gonzalo Martínez-Muñoz. A comparative analysis of gradient boosting algorithms. *Artificial Intelligence Review*, 54:1937–1967, 2021.
- [14] Ravid Shwartz-Ziv and Amitai Armon. Tabular data: Deep learning is not all you need. *Information Fusion*, 81:84–90, 2022.
- [15] Jerome H. Friedman. Greedy function approximation: A gradient boosting machine. *The Annals of Statistics*, 29(5):1189–1232, 2001.
- [16] Tianqi Chen and Carlos Guestrin. Xgboost: A scalable tree boosting system. In *Proceedings of the 22nd ACM SIGKDD International Conference on Knowledge Discovery and Data Mining, KDD '16*, pages 785–794, New York, NY, USA, 2016. Association for Computing Machinery.
- [17] Liudmila Prokhorenkova, Gleb Gusev, Aleksandr Vorobev, Anna Veronika Dorogush, and Andrey Gulin. Catboost: unbiased boosting with categorical features. In *Advances in Neural Information Processing Systems*, volume 31. Curran Associates, Inc., 2018.

- [18] Guolin Ke, Qi Meng, Thomas Finley, Taifeng Wang, Wei Chen, Weidong Ma, Qiwei Ye, and Tie-Yan Liu. Lightgbm: A highly efficient gradient boosting decision tree. In *Advances in Neural Information Processing Systems 30: Annual Conference on Neural Information Processing Systems 2017, December 4-9, 2017, Long Beach, CA, USA*, pages 3146–3154, 2017.
- [19] Wei Zhang, Xianhui Liu, Yi Ding, and Deming Shi. Multi-output ls-svr machine in extended feature space. In *2012 IEEE International Conference on Computational Intelligence for Measurement Systems and Applications (CIMSA) Proceedings*, pages 130–134, 2012.
- [20] Sven Peter, Ferran Diego, Fred A. Hamprecht, and Boaz Nadler. Cost efficient gradient boosting. In *Advances in Neural Information Processing Systems 30: Annual Conference on Neural Information Processing Systems 2017, December 4-9, 2017, Long Beach, CA, USA*, pages 1551–1561, 2017.
- [21] Haihao Lu, Sai Praneeth Karimireddy, Natalia Ponomareva, and Vahab S. Mirrokni. Accelerating gradient boosting machines. In *The 23rd International Conference on Artificial Intelligence and Statistics, AISTATS 2020, 26-28 August 2020, Online [Palermo, Sicily, Italy]*, volume 108 of *Proceedings of Machine Learning Research*, pages 516–526. PMLR, 2020.
- [22] Ezgi Zorarpaci. A fast intrusion detection system based on swift wrapper feature selection and speedy ensemble classifier. *Engineering Applications of Artificial Intelligence*, 133:108162, 2024.
- [23] Lifeng Huang, Qiong Huang, Peichao Qiu, Shuxin Wei, and Chengying Gao. Fasten: Fast ensemble learning for improved adversarial robustness. *IEEE Transactions on Information Forensics and Security*, 19:2565–2580, 2024.
- [24] Hanen Borchani, Gherardo Varando, Concha Bielza, and Pedro Larrañaga. A survey on multi-output regression. *WIREs Data Mining and Knowledge Discovery*, 5(5):216–233, 2015.
- [25] Eleftherios Spyromitros-Xioufis, Grigorios Tsoumakas, William Groves, and Ioannis Vlahavas. Multi-target regression via input space expansion: treating targets as inputs. *Machine Learning*, 104(1):55–98, Jul 2016.
- [26] Eleftherios Spyromitros-Xioufis, Konstantinos Sechidis, and Ioannis Vlahavas. Multi-target regression via output space quantization. In *2020 International Joint Conference on Neural Networks (IJCNN)*, pages 1–9, 2020.
- [27] Natalia Ponomareva, Thomas Colthurst, Gilbert Hendry, Salem Haykal, and Soroush Radpour. Compact multi-class boosted trees. In *2017 IEEE International Conference on Big Data (Big Data)*, pages 47–56, 2017.
- [28] Zhendong Zhang and Cheolkon Jung. Gbdt-mo: Gradient-boosted decision trees for multiple outputs. *IEEE Transactions on Neural Networks and Learning Systems*, 32(7):3156–3167, 2021.
- [29] Yoav Freund and Robert E Schapire. A decision-theoretic generalization of on-line learning and an application to boosting. *Journal of computer and system sciences*, 55(1):119–139, 1997.
- [30] Llew Mason, Peter L. Bartlett, and Jonathan Baxter. Direct optimization of margins improves generalization in combined classifiers. In *Advances in Neural Information Processing Systems 11, [NIPS Conference, Denver, Colorado, USA, November 30 - December 5, 1998]*, pages 288–294. The MIT Press, 1998.
- [31] Llew Mason, Jonathan Baxter, Peter L Bartlett, Marcus Frean, et al. Functional gradient techniques for combining hypotheses. *Advances in Neural Information Processing Systems*, pages 221–246, 1999.
- [32] Jerome H. Friedman and Jacqueline J. Meulman. Multiple additive regression trees with application in epidemiology. *Statistics in Medicine*, 22(9):1365–1381, 2003.
- [33] Günther Eibl and Karl Peter Pfeiffer. Multiclass boosting for weak classifiers. *Journal of Machine Learning Research*, 6:189–210, 2005.
- [34] Jerome Friedman, Trevor Hastie, and Robert Tibshirani. Additive logistic regression: a statistical view of boosting (With discussion and a rejoinder by the authors). *The Annals of Statistics*, 28(2):337 – 407, 2000.
- [35] Ping Li. Abc-boost: adaptive base class boost for multi-class classification. In *Proceedings of the 26th Annual International Conference on Machine Learning, ICML '09*, pages 625–632, New York, NY, USA, 2009. Association for Computing Machinery.
- [36] Xingbin Zhan, Shuaichao Zhang, Wai Yuen Szeto, and Xiqun Chen. Multi-step-ahead traffic speed forecasting using multi-output gradient boosting regression tree. *Journal of Intelligent Transportation Systems*, 24(2):125–141, 2020.
- [37] Hendrik Blockeel, Luc De Raedt, and Jan Ramon. Top-down induction of clustering trees. In *Proceedings of the Fifteenth International Conference on Machine Learning (ICML 1998), Madison, Wisconsin, USA, July 24-27, 1998*, pages 55–63. Morgan Kaufmann, 1998.
- [38] Jan Struyf and Sašo Džeroski. Constraint based induction of multi-objective regression trees. In *Knowledge Discovery in Inductive Databases*, pages 222–233, Berlin, Heidelberg, 2006. Springer Berlin Heidelberg.

- [39] Leo Breiman, J. H. Friedman, Richard A. Olshen, and C. J. Stone. *Classification and Regression Trees*. Wadsworth, Oxfordshire, UK, 1984.
- [40] Dragi Kocev, Celine Vens, Jan Struyf, and Sašo Džeroski. Ensembles of multi-objective decision trees. In *Machine Learning: ECML 2007*, pages 624–631, Berlin, Heidelberg, 2007. Springer Berlin Heidelberg.
- [41] Leo Breiman. Bagging predictors. *Machine Learning*, 24(2):123–140, Aug 1996.
- [42] Leo Breiman. Random forests. *Machine Learning*, 45(1):5–32, 10 2001.
- [43] Felipe Kenji Nakano, Konstantinos Pliakos, and Celine Vens. Deep tree-ensembles for multi-output prediction. *Pattern Recognition*, 121:108211, 2022.
- [44] Jerome H. Friedman. Stochastic gradient boosting. *Computational Statistics & Data Analysis*, 38(4):367–378, 2002. Nonlinear Methods and Data Mining.
- [45] Isabelle M Guyon. Design of experiments for the nips 2003 variable selection benchmark. 2003. Last visited on April 28, 2024.
- [46] Alex Krizhevsky, Vinod Nair, and Geoffrey Hinton. Cifar-10 (canadian institute for advanced research). 2009. Last visited on April 28, 2024.
- [47] Markelle Kelly, Rachel Longjohn, and Kolby Nottingham. The uci machine learning repository. <https://archive.ics.uci.edu>. Last accessed on April 28, 2024.
- [48] Li Deng. The mnist database of handwritten digit images for machine learning research [best of the web]. *IEEE Signal Processing Magazine*, 29(6):141–142, 2012.
- [49] Marco F Duarte and Yu Hen Hu. Vehicle classification in distributed sensor networks. *Journal of Parallel and Distributed Computing*, 64(7):826–838, 2004. Computing and Communication in Distributed Sensor Networks.
- [50] Janez Demšar. Statistical comparisons of classifiers over multiple data sets. *The Journal of Machine Learning Research*, 7:1–30, 2006.